



IX International Macromolecular
Colloquium

306628



6º CONGRESSO BRASILEIRO DE POLÍMEROS

IX INTERNATIONAL MACROMOLECULAR COLLOQUIUM

11 a 15 de novembro de 2001
Centro de Convenções do Hotel Serrano
Gramado/RS

Promoção:



Associação Brasileira de Polímeros

Instituto de Química da Universidade
Federal do Rio Grande do Sul (IQ/UFRGS)

PROPERTIES AND MECHANISTIC ASPECTS OF PLASTIC DEFORMATION IN THE ISOTACTIC POLYPROPYLENE



Shinichi Tokumoto¹ and Dimitrios Samios^{2*}

¹Centro de Tecnologia OPP Química III Pólo Petroquímico, Via Oeste Lote 05, Passo Raso 95853-000 Triunfo – RS
tokumoto@opp.com.br;

²Instituto de Química da UFRGS, Av. Bento Gonçalves, 9500 Caixa Postal 15003, Agronomia 91501-970 Porto Alegre - RS dsamios@if.ufrgs.br

Plane strain compression performed between T_g and T_m in the isotactic polypropylene is discussed in terms of morphology change, stress relaxation and final properties of plastically deformed specimens. For each one of the three well defined regions in the stress – strain curve, a discussion is presented, as well as the influence of processing conditions as strain ratio, strain rate and temperature. Notoriously, T_{α_c} transition is strongly enhanced in the deformed samples. A model for structural array of deformed material, which involves additional interface layer between crystalline lamellae and amorphous phase, is proposed in order to find out a consistent agreement among DSC, DMA and x-ray diffraction analyses.

Introduction

Investigations about mechanisms of plastic deformation on thermoplastic polymers were remarkable by the beginning of seventies [1,2,3]. In the last decades, due to developments of processing technologies and requirements of enhanced mechanical properties of final goods, further studies were carried out [4,5,6,] and a comprehensive knowledge about microstructure of the plastically deformed polymers have been collected over the years [4,5,7,8].

However, industrial practice did not follow scientific advances in this field, even though several advantages as increase of transparency, strength and rigidity have been pointed out in the highly deformed materials [9]. Thus, in order to make plastic deformation technique easily applicable in the industrial field, this study tries to bring additional contribution in this subject, as correlation between structure and rheological properties of the polymers during plastic deformation, which is still not well established. The compression test in a channel die [3, 6,10] allows monoaxial flow without internal cavitation [10]. Moreover, specimens prepared so, their deformation can provide a single crystal like texture, with c -axis being oriented along the flow direction, the a -axis along the loading direction, and the b -axis along the constraint direction [6], a helpful design for better understanding of the physical phenomena.

In the present report, structural effects on stress-strain curve are discussed for isotactic polypropylene samples, as well as the main features and properties of plastically deformed specimens in a channel die.

Experimental

Plane-Strain Compression in the Channel Die

Injection molded bars of different molecular weight PP samples were annealed at 140°C and 6 hours under nitrogen. The specimen, with dimensions of 6.35 mm x 12.50 mm x 100.00 mm was laid in the channel of the die and over it was placed the plunger, just as showed in Figure 1.

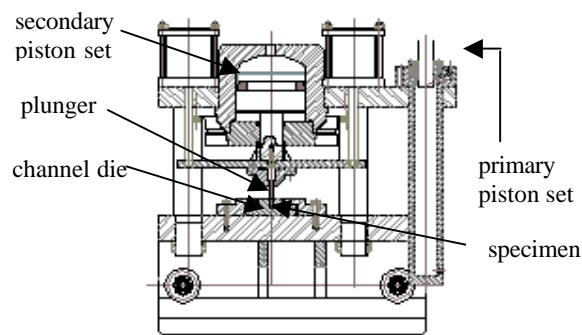


Figure 1: Force amplifier and assembling scheme for compression test in the channel die.

After at least 20 minutes for temperature equalization between specimen and die, the compression was carried out according to Figure 1. The plunger was pulled down by secondary piston of the force amplifier, which is activated with transmission fluid compressed by primary piston. The later was assembled to the Instron® Model 4466 dynamometer, which has highly accurate displacement, speed and load control and data collection. Detailed description of the force amplifier and necessary correction curves can be found elsewhere [11].

Measurements

Deformed bars were analyzed by modulated DSC TA Instruments model MDSC 2920. First heating was performed from -40°C to 200°C at $5^{\circ}\text{C}/\text{min}$ ramp and modulation amplitude of $\pm 0.80^{\circ}\text{C}$ every 60 s.

DMA tests were performed in the Dynamic Mechanical Analyzer DuPont model 983, using a 2 mm thick bars deformed at several compression ratios. Scanning was performed at 1 Hz oscillation and $2^{\circ}\text{C}/\text{min}$ heating rate from -50°C to 130°C or up to mechanical collapse.

Density values were determined sinking a piece of specimen into a gradient column, prepared with a suitable mixture between isopropyl alcohol and water to set density range from 0.8998 g/cc to 0.9238 g/cc. The column was kept at $23^{\circ}\text{C} \pm 0.1^{\circ}\text{C}$.

Crystallographic planes of iPP crystallites in the deformed samples was examined by means of wide-angle X-ray diffractometer Rigaku model D/MAX-2100 consisting of the Ultima+ theta-theta goniometer coupled to sealed anode X-ray generator operating at 40 kV and 20 mA (Cu $K\alpha$), equipped with NaI cintilation detector.

Results and Discussion

The rheological and mechanical behavior of deformed samples come from several changes on microstructure occurred during the plastic flow. The Figure 2 reports a typical stress – plane strain compression ratio curves. Three different regions can be identified in the plot. The first region corresponding to low deformation level shows a quite good linearity between strain and imposed stress. In the end of this region the material starts to yield and reaches the plateau, which was indicated as second region. Yielding strain was independent to the molecular weight of the sample and started at compression ratio (CR) of about 5.5%. The transition between elastic and inelastic response involves the occurrence of relative displacement among chain segments and it starts in the weaker points, i. e., in the amorphous phase of the material. Hence, the independence of molecular weight can be attributed to morphological response instead of molecular structure response. The plateau in the second region covers a quite extensive deformation range.

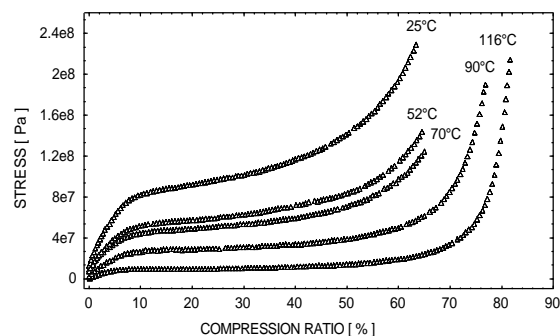


Figure 2: Stress – compression ratio curves of the sample H5 ($M_w = 419800$, $M_w/M_n = 7.6$), run at several temperatures and 1,8 mm/min rate.

Roughly, starts about 10% strain and goes up to $\sim 50\%$ strain depending on sample and processing conditions. The plateau ends when stress starts to increase drastically, going into third region. The slope of the curve in the later almost reaches infinity. At that point material collapses by fragmentation and releases an explosion noise. The phenomenon is understood as the release of elastic energy stored during the whole plastic deformation process. Intriguingly, stress curves in Figure 2 converge to a certain limiting value of stress and compression ratio. Extrapolation of the curves guided to a stress range of 0.205 GPa to 0.245 GPa and a compression ratio of 77% to 83%.

In the beginning of shear compression, the applied load causes soft changes on the morphology without modifying the configuration of interactive field between amorphous and crystalline components. In other words, the prevalent elastic response is related to the energy stored in the spherulitic morphology level. The Figure 3 can support this statement. The increase of molecular weight demands lower load in the material yielding. When shear stress is applied on the spherulites, equatorial region undergoes yielding preferentially [12]. Concurrently, the size of spherulites increases when molecular weight is diminished for a similar crystallization history. The spherulites growth rate decreases with increasing average molecular weight [13] due to longer reptation time.

In the rheological point of view, we can consider that amorphous phase makes the matrix role in the flow system whereas crystalline part behaves as solid charge immersed into it. The viscosity, expressed here indirectly as stress, increases as spherulite size increases (low molecular weight sample), comparing samples with about the same crystallinity. By the other hand, if the spherulites are considered as blend component with very high viscosity, it undergoes less shear than the whole material [14]. This leads that spherulites breaking by shear becomes more difficult as the viscosity of the medium is lowered and thus, the plateau gets higher stress level, just as happened with sample H2 in Figure 3. The existence of a plateau in the curve reveals that the flow activation energy is not altered in a certain range of deformation even that morphology changes occur along the process. One evidence for this is the decrease of crystallinity of the

specimen with CR, reported in Figure 4 in terms of density.

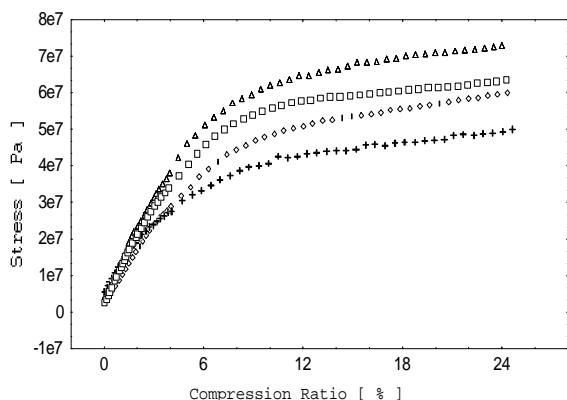


Figure 3: Stress – plane strain compression curves at 52°C and 1,8 mm/min rate of samples H2 (triangle; Mw = 228600), H5 (square; Mw=419800), H6 (diamond; Mw=448400) and H9 (cross; Mw=708900). Mw/Mn ranged between 6.6 and 7.6.

Significant density decrease began around 25% of CR. The crystallites suffer their massive destruction progressively and monotonically from plateau region to final zone.

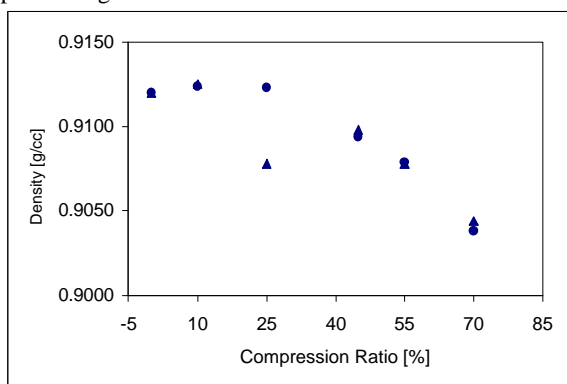


Figure 4: Density values for sample H5 submitted to different plane strain compression at 25°C (triangle) and 52°C (circle) and 1,8 mm/min.

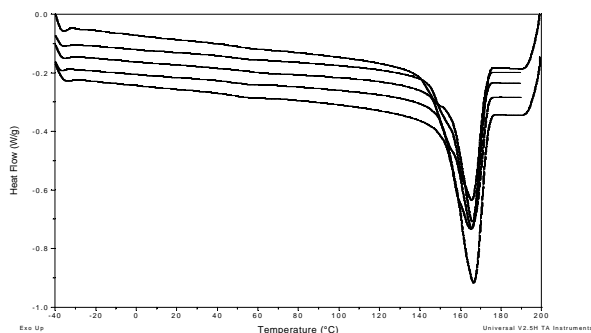


Figure 5: Conventional first heating DSC thermograms of sample H5. Specimens deformed at 25°C and 1,8 mm/min with nominal compression ratio of 0%, 10%, 25%, 45% and 55%, respectively, from the upper to the lower curve.

First run DSC thermograms revealed that crystallite destruction obeys a certain selectivity, as

reported in Figures 5 and 6. The later plot, that expresses the relative amount of defective crystals and low melting crystallites as β form, reports a preferential disappearance of this species with CR. The stable value for Qp/Qt ratio coincides with the beginning of density decrease in Figure 4. Thus, it is believed that strong morphological change occurs beyond this point at lamellae level, in a further step of spherulites fragmentation.

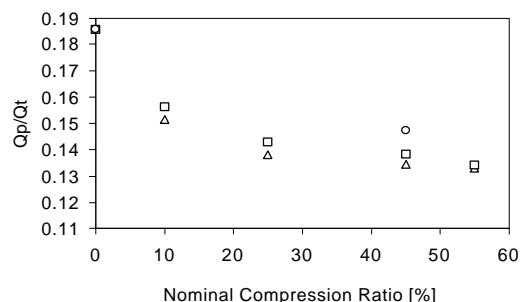


Figure 6: Enthalpy ratio between heat absorbed up to 148°C and total melting heat of sample H5. Specimens were deformed at 25°C (triangle), 52°C (square) and 90°C (circle) and 1,8 mm/min compression rate.

Another important feature of plastically deformed PP is the enhancement of $T\alpha_c$ [15,16] transition with CR, thermally observable by non reversible MDSC curves in Figure 7.

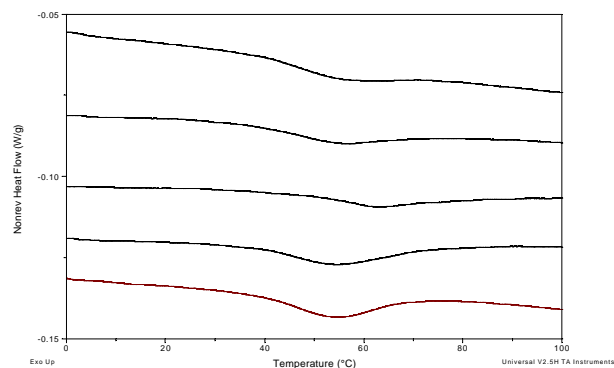
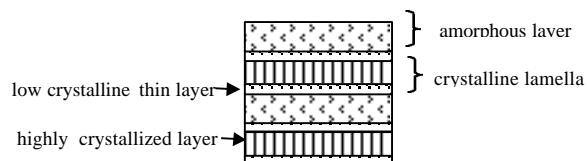


Figure 7: Non reversible DSC curves from modulated heating of sample H5. Specimens deformed at 25°C and 1,8 mm/min, nominal compression ratio of 0%, 10%, 25%, 45% and 55%, respectively, from the upper to the lower curve.

The endothermic character of this transition suggests a “melting like” transition to disentangle highly oriented amorphous moieties. But one could expect exothermic behavior due to frictional energy produced by stress release and consequent entropy increase. A reasonable explanation is demonstrated in the model proposed in the Scheme 1. During the plastic flow, crystalline ribbons undergo severe mechanical shear and their surfaces are highly damaged. Thus, a loosely ordered thin layer, which had negligible effect before, starts to develop significant

role in the material property. Following, lamella thickness of the crystalline layer should be reduced.



Scheme 1: Proposed structure for plastically deformed semi-crystalline polymers.

X-ray diffraction analysis provided us indicatives of lamella thinning with CR increase through increase of β value in Figure 8. Calculations of β value and s value are described elsewhere [17]. However, the plot help us to notice that higher the β value, thinner is the lamella and higher the slope, more deformed is the crystallographic unit cell.

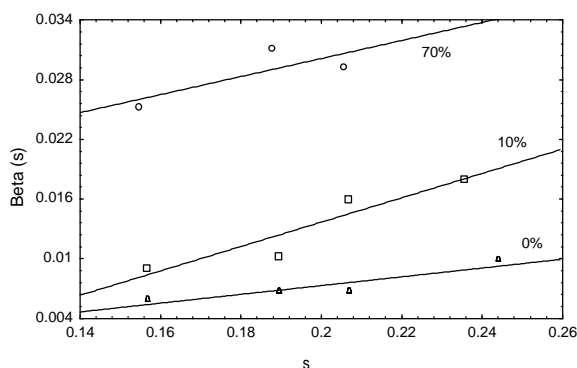


Figure 8: $\beta(s)$ vs. s plot from wide angle X-ray diffractogram analyzed in the constrained side of the sample H5, which was deformed at 70°C and 1.8 mm/min. Nominal compression ratio 00% (triangle), 10% (square) and 70% (circle).

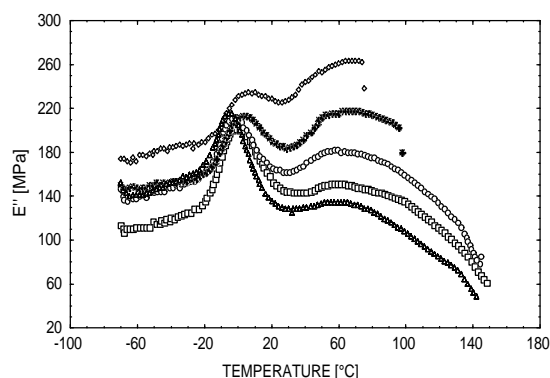


Figure 9: Loss modulus from DMA for sample H1 ($M_w=161800$), plastically deformed at 52°C and 1.8 mm/min. Nominal compression ratio 00% (triangle), 10% (square), 25% (circle), 45% (star) and 55% (diamond).

T_{α_c} transition was also confirmed by DMA analysis. Dynamic responses showed proportional increase of this transition with CR as reported in Figure 9. Its maximum stayed around 80°C in agreement with literature [15]. The starting temperature matched with DSC results in around 55°C.

Conclusion

Plastic deformation performed by plane strain compression provided three well defined zones in the stress-strain curve. Deformed specimens revealed high loss modulus in the dynamic mechanical tests. Thermal data indicated a selective destruction of crystallites during the processing and the enhancement of T_{α_c} transition. The model proposed for structure of plastically deformed semi-crystalline polymers extended the definition of T_{α_c} to lamella surface aggregates. Normally, it's referred only for inside defects [15].

Acknowledgements

Acknowledgements are made to FAPERGS and PADCT for sponsoring this research. OPP Química S.A. is acknowledged for financial support to build the Force Amplifier and for all tests and analyses performed at the Technology Center.

References

1. Peterlin, A.; *J. of Mat. Sci.*, 1971, 6, 490.
2. Shinozaki, D. M. and Groves, G. W.; *J. of Mat. Sci.*, 1973, 8, 1012.
3. Young, R. J., Bowden, P. B., Ritchie, J. M. and Rider, J. G.; *J. of Mat. Sci.*, 1973, 8, 23.
4. Galeski, A.; Argon, A. S. and Cohen, R. E.; *Macromolecules*, 1988, 21, 2761.
5. Bartzak, Z.; Argon and Cohen, R. E.; *Polymer*, 1994, 35, 3427.
6. Bartzak, Z.; Argon, A. S. and Cohen, R. E.; *Macromolecules*, 1992, 25, 5036.
7. Galeski, A.; Argon, A. S. and Cohen, R. E.; *Makromol. Chem.*, 1987, 188, 1195.
8. Wu, G.; Tucker, P. A. and Cuculo, J. A.; *Polymer*, 1997, 38, 1091.
9. Beresnev, B. I., Shishkova, N. V. and Tsygankov, S. A.; *Physica*, 1986, 139&140B, 629.
10. Bartzak, Z.; Galeski, A.; Argon, A. S. and Cohen, R. E.; *Polymer*, 1996, 37(11), 2113.
11. Tokumoto, S., Samios, D. and Bragança, A. L. D.; BR Patent deposit MU7903031-9, 1999.
12. Lin, L. and Argon, A. S.; *J. Mater. Sci.*, 1994, 29, 294.
13. De Carvalho, B. and Bretas, R. E. S.; *J. of Appl. Polym. Sci.*, 1998, 68, 1159.
14. Bretas, R. E. S. and D'Avila, M. A.; *Reologia de Polímeros Fundidos*, EdUFSCar – Editora da Univ. Federal de São Carlos, São Paulo, 2000.
15. Rault, J.; *J.M.S.- Rev. Macromol. Chem. Phys.*, 1997, C37(2), 335.
16. Botey, M., Neffati, R. and Rault, J.; *Polymer*, 1999, 40, 5227.
17. Klug, H. P. and Alexander, L. E.; “X-Ray Diffraction Procedures”, Second Ed., John Wiley & Sons, Inc., 1974.

